



Corrosion processes at the GGG40 steel–bentonite interface

Andrés G. Muñoz¹ and Dieter Schild²

¹Repository Research, Gesellschaft für Anlagen und Reaktorsicherheit (GRS gGmbH),
38122 Braunschweig, Germany

²Institute for Nuclear Disposal, Karlsruhe Institute of Technology (KIT),
76344 Eggenstein-Leopoldshafen, Germany

Correspondence: Andrés G. Muñoz (andres.munoz@grs.de)

Received: 30 March 2023 – Revised: 21 June 2023 – Accepted: 23 June 2023 – Published: 6 September 2023

Abstract. Spheroidal graphite cast iron (GGG40/0.7040) is used as an overpack material for the reference Pol-lux 10 container, a prototype for the storage of fuel elements in different types of host rocks (Hassel et al., 2019). Corrosion processes are expected to be triggered after some decades, as the contacting bentonite, which is used as fill material, becomes soggy because of the decay of the fission heat generation and the intrusion of pore water as the temperature decreases under the condensation point (King and Padovani, 2011). The distinct electrochemical reactivities of the graphite, ferrite, pearlite, and cementite phases exposed by this material introduce local galvanic elements which influence the topographic evolution of degradation (Spence, 2005). The aim of this work is to elucidate the corrosion dynamics of active and passive areas by following the chemical evolution at the interface of cast iron–bentonite during the first stages after its saturation with geological pore water. Polarization experiments and electrochemical impedance spectroscopy were applied to monitor the corrosion process in a bentonite cell, where GGG40 steel is put into contact with a light compacted Wyoming bentonite slurry 1 : 10 *w/w* of bentonite to Opalinus Clay pore water (Fig. 1a). Experiments were performed at 30 and 50 °C for longer than 3 months. The surface chemistry and morphological changes were investigated by local XPS, SEM-EDX, and TEM (X-ray photoelectron spectroscopy, scanning electron microscopy with energy dispersive X-ray, and transmission electron microscopy, respectively). These experiments were complemented with corrosion studies performed in pore water under different temperatures, hydrostatic pressures, and pH and with and without dissolved oxygen.

The polarization curves indicate a constant corrosion rate of GGG40 steel in saturated bentonite after 30 d. SEM micrographs reveal a preferential dissolution of the ferrite phase around the graphite spheres and the ferrite lamellae contained in the pearlitic eutectic. A strong localized dissolution of ferrite along the graphite boundary can be also observed; this is a typical case of crevice corrosion caused by the unhindered access of oxygen to the graphitic cathodic areas (Wang et al., 2022). The surface chemical studies indicate the accumulation of iron oxides, which can be attributed to a hydrated magnetite and the formation of iron silicates (Zhang et al., 2021). TEM pictures of a cross-sectional lamella, including part of graphite sphere, show the formation of a silicate film covering the corroding surface with an irregular adherence (Fig. 1b).

The initial relatively high corrosion rate of GGG40 steel can be attributed to the dissolution of the more active ferrite with the formation of poorly passivating iron oxides and silicates. The system is driven towards the dissolution of pearlite at more positive electrode potentials. The bentonite slurry limits the access of oxygen to the graphitic cathodic areas, reducing the corrosion rate by 1 order of magnitude in comparison with that in aerated pore water. A surface enrichment of cementite with superior passive properties and the neutralization of the local elements by approaching the corrosion potential of graphite (Kadowaki et al., 2019) is also expected. Thus, the consumption of oxygen and the transport limitation of the cathodic reaction by bentonite forecast a considerable reduction in the degradation of the container after a sacrificial corrosion phase.

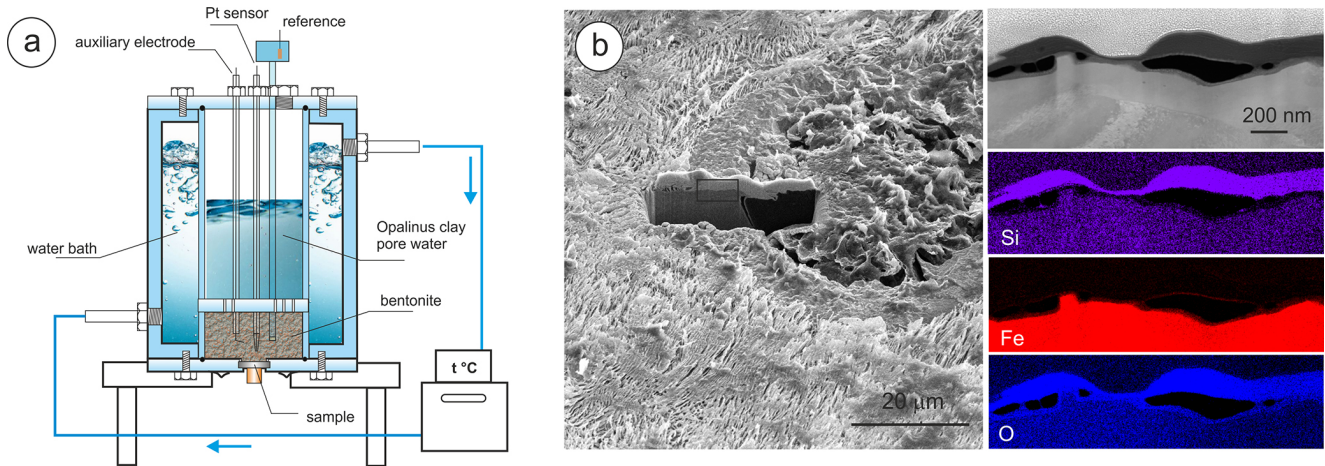


Figure 1. (a) Schematic representation of the bentonite-cell. (b) SEM picture of the surface of GGG40 steel after 3 months of corrosion when in contact with saturated bentonite. The images on the right of panel (b) show the TEM of an interfacial cross section with EDX analysis.

Data availability. The data that support the findings of this study are available from the corresponding author (Andrés G. Muñoz) upon reasonable request.

Author contributions. AGM: data interpretation, writing, and investigation. DS: data interpretation and investigation.

Acknowledgements. The Federal Ministry for Environment, Nature Conservation, Nuclear Safety and Consumer Protection (BMUV; grant no. 02 E 11981A) and the European Union's Horizon 2020 research programme (grant no. 847593) are gratefully acknowledged for the funding of this work.

Financial support. This research has been supported by the Bundesministerium für Umwelt, Naturschutz und Reaktorsicherheit (BMUV; grant no. 02 E 11981A) and the European Union's Horizon 2020 research programme (grant no. 847593).

References

- Hassel, T., Köhler, A., and Kurt, Ö. S.: Das ENCON-Behälterkonzept – Generische Behältermodelle zur Einlagerung radioaktiver Reststoffe für den interdisziplinären Optionsvergleich, ENTRIA-Arbeitsbericht-16, Institut für Werkstoffe, Leibniz-Universität Hannover, Hannover, Germany, ISSN 2367-3532, 2019.
- Kadowaki, M., Muto, I., Takahashi, K., Doi, T., Masuda, H., Katayama, H., Kawano, K., Sugawara, Y., and Hara, N.: Anodic polarization characteristics and electrochemical properties of Fe₃C in chloride solutions, *J. Electrochem. Soc.*, 166, C345–C351, 2019.
- King, F. and Padovani, C.: Review of the corrosion performance of selected canister materials for disposal of UK HLW and/or spent fuel, *Corros. Eng. Sci. Technol.* 46, 82–90, 2011.
- Spence, T. C.: Corrosion of cast iron, *ASM Handbook*, Vol. 13B: Corrosion: Materials, edited by: Cramer, S. D. and Covino Jr., B. S., ASM, Materials Park, Ohio, 43–50, ISBN 0-87170-707-1, 2005.
- Wang, B., Liu, T., Tao, K., Zhu, L., Liu, C., Yong, X., and Cheng, X.: A study of the mechanisms and kinetics of the localized corrosion aggravation of ductile iron in a Harsh water quality environment, *Metals*, 12, 2103, <https://doi.org/10.3390/met12122103>, 2022.
- Zhang, Y., Xiao, J., Zhang, Y., Liu, W., Pei, W., Zhao, A., Zhang, W., and Zeng, L.: The study on corrosion behavior and corrosion resistance of ultralow carbon high silicon iron-based alloy, *Mater. Res. Express*, 8, 026504, <https://doi.org/10.1088/2053-1591/abdc52>, 2021.